JOURNAL OF Applied Polymer SCIENCE

Special Issue: Bio-based Packaging

Guest Editors: José M. Lagarón, Amparo López-Rubio, and María José Fabra
Institute of Agrochemistry and Food Technology of the Spanish Council for Scientific Research

EDITORIAL

REVIEWS

RESEARCH ARTICLES

JOURNAL OF Applied Polymer SCIENCE

Special Issue: Bio-based Packaging

Guest Editors: José M. Lagarón, Amparo López-Rubio, and María José Fabra
Institute of Agrochemistry and Food Technology of the Spanish Council for Scientific Research

Impact of fermentation residues on the thermal, structural, and rheological properties of polyhydroxy(butyrate-*co*-valerate) produced from cheese whey and olive oil mill wastewater
L. Hilliou, D. Machado, C. S. S. Oliveira, A. R. Gouveia, M. A. M. Reis, S. Campanari, M. Villano and M. Majone, *J. Appl. Polym. Sci.* 2015, DOI: 10.1002/app.42818

Synergistic effect of lactic acid oligomers and laminar graphene sheets on the barrier properties of polylactide nanocomposites obtained by the in situ polymerization pre-incorporation method
J. Ambrosio-Martín, A. López-Rubio, M. J. Fabra, M. A. López-Manchado, A. Sorrentino, G. Gorrasi and J. M. Lagarón, *J. Appl. Polym. Sci.* 2015, DOI: 10.1002/app.42661

Antibacterial poly(lactic acid) (PLA) films grafted with electrospun PLA/allyl isothiocyanate fibers for food packaging
H. H. Kara, F. Xiao, M. Sarker, T. Z. Jin, A. M. M. Sousa, C.-K. Liu, P. M. Tomasula and L. Liu, *J. Appl. Polym. Sci.* 2015, DOI: 10.1002/app.42475

Poly(L-lactide)/ZnO nanocomposites as efficient UV-shielding coatings for packaging applications
E. Lizundia, L. Ruiz-Rubio, J. L. Vilas and L. M. León, *J. Appl. Polym. Sci.* 2015, DOI: 10.1002/app.42426

Effect of electron beam irradiation on the properties of polylactic acid/montmorillonite nanocomposites for food packaging applications
M. Salvatore, A. Marra, D. Duraccio, S. Shayanfar, S. D. Pillai, S. Cimmino and C. Silvestre, *J. Appl. Polym. Sci.* 2015, DOI: 10.1002/app.42219

Preparation and characterization of linear and star-shaped poly L-lactide blends
M. B. Khajeheian and A. Rosling, *J. Appl. Polym. Sci.* 2015, DOI: 10.1002/app.42231

Mechanical properties of biodegradable polylactide/poly(ether-block-amide)/thermoplastic starch blends: Effect of the crosslinking of starch
L. Zhou, G. Zhao and W. Jiang, *J. Appl. Polym. Sci.* 2015, DOI: 10.1002/app.42297

Interaction and quantification of thymol in active PLA-based materials containing natural fibers
I. S. M. A. Tawakkal, M. J. Cran and S. W. Bigger, *J. Appl. Polym. Sci.* 2015, DOI: 10.1002/app.42160

Graphene-modified poly(lactic acid) for packaging: Material formulation, processing, and performance
M. Barletta, M. Puopolo, V. Tagliaferri and S. Vesco, *J. Appl. Polym. Sci.* 2015, DOI: 10.1002/app.42252

Edible films based on chia flour: Development and characterization
M. Dick, C. H. Pagno, T. M. H. Costa, A. Gomaa, M. Subirade, A. De O. Rios and S. H. Flóres, *J. Appl. Polym. Sci.* 2015, DOI: 10.1002/app.42455

Influence of citric acid on the properties and stability of starch-polycaprolactone based films
R. Ortega-Toro, S. Collazo-Bigliardi, P. Talens and A. Chiralt, *J. Appl. Polym. Sci.* 2015, DOI: 10.1002/app.42220

Bionanocomposites based on polysaccharides and fibrous clays for packaging applications
A. C. S. Alcântara, M. Darder, P. Aranda, A. Ayral and E. Ruiz-Hitzky, *J. Appl. Polym. Sci.* 2015, DOI: 10.1002/app.42362

Hybrid carrageenan-based formulations for edible film preparation: Benchmarking with kappa carrageenan
F. D. S. Larotonda, M. D. Torres, M. P. Gonçalves, A. M. Sereno and L. Hilliou, *J. Appl. Polym. Sci.* 2015, DOI: 10.1002/app.42263

JOURNAL OF Applied Polymer SCIENCE

Special Issue: Bio-based Packaging

Guest Editors: José M. Lagarón, Amparo López-Rubio, and María José Fabra
Institute of Agrochemistry and Food Technology of the Spanish Council for Scientific Research

Structural and mechanical properties of clay nanocomposite foams based on cellulose for the food packaging industry
S. Ahmadzadeh, J. Keramat, A. Nasirpour, N. Hamdami, T. Behzad, L. Aranda, M. Vilasi and S. Desobry, *J. Appl. Polym. Sci.* 2015, DOI: 10.1002/app.42079

Mechanically strong nanocomposite films based on highly filled carboxymethyl cellulose with graphene oxide
M. El Achaby, N. El Miri, A. Snik, M. Zahouily, K. Abdelouahdi, A. Fihri, A. Barakat and A. Solhy, *J. Appl. Polym. Sci.* 2015, DOI: 10.1002/app.42356

Production and characterization of microfibrillated cellulose-reinforced thermoplastic starch composites
L. Lendvai, J. Karger-Kocsis, Á. Kmetty and S. X. Drakopoulos, *J. Appl. Polym. Sci.* 2015, DOI: 10.1002/app.42397

Development of bioplastics based on agricultural side-stream products: Film extrusion of *Crambe abyssinica*/wheat gluten blends for packaging purposes
H. Rasel, T. Johansson, M. Gällstedt, W. Newson, E. Johansson and M. Hedenqvist, *J. Appl. Polym. Sci.* 2015, DOI: 10.1002/app.42442

Influence of plasticizers on the mechanical and barrier properties of cast biopolymer films
V. Jost and C. Stramm, *J. Appl. Polym. Sci.* 2015, DOI: 10.1002/app.42513

The effect of oxidized ferulic acid on physicochemical properties of bitter vetch (*Vicia ervilia*) protein-based films
A. Arabestani, M. Kadivar, M. Shahedi, S. A. H. Goli and R. Porta, *J. Appl. Polym. Sci.* 2015, DOI: 10.1002/app.42894

Effect of hydrochloric acid on the properties of biodegradable packaging materials of carboxymethylcellulose/poly(vinyl alcohol) blends
M. D. H. Rashid, M. D. S. Rahaman, S. E. Kabir and M. A. Khan, *J. Appl. Polym. Sci.* 2015, DOI: 10.1002/app.42870

Journal of Applied Polymer Science

Effect of electron beam irradiation on the properties of polylactic acid/montmorillonite nanocomposites for food packaging applications

Marcella Salvatore,[1] Antonella Marra,[1] Donatella Duraccio,[1] Shima Shayanfar,[2] Suresh D. Pillai,[2] Sossio Cimmino,[1] Clara Silvestre[1]

[1]Institute of Polymers, Composites and Biomaterials CNR, Pozzuoli Naples, Italy
[2]National Center for Electron Beam Research, Texas A&M University, Texas
Correspondence to: C. Silvestre (E-mail: silvestre@ictp.cnr.it)

ABSTRACT: This study was aimed at (1) developing new films based on polylactic acid/montmorillonite (PLA/MMT) with improved properties for applications in the food packaging industry and (2) analyzing the effect of electron-beam (eBeam) radiation on the structural, morphological, mechanical, and barrier properties of these nanomaterials. Nanocomposites based on PLA with 1, 3, and 5 wt % of MMT were prepared in a twin-screw extruder and then filmed by a calender. The nanocomposites were exposed to eBeam doses; one set at 1 kGy dose and the other at 10 kGy dose. The effect of MMT addition and of eBeam radiation on the properties of PLA were assessed. For all composites, a homogeneous distribution and dispersion of MMT in the PLA matrix was obtained. All nanocomposites showed an increase of the mechanical and oxygen-barrier properties compared to neat PLA. The eBeam irradiation caused an increase of the crystallinity, formation of crosslink, increase of the glass-transition temperatures, and enhancement of the yield values in the stress–strain curves for all nanocomposites. This study demonstrated that PLA/MMT films are suitable materials for eBeam processing of prepacked food at the realistic doses that were employed in this study. © 2015 Wiley Periodicals, Inc. J. Appl. Polym. Sci. **2016**, *133*, 42219.

KEYWORDS: biopolymers and renewable polymers; clay; nanostructured polymers; packaging; property relations; structure

Received 16 January 2015; accepted 9 March 2015
DOI: 10.1002/app.42219

INTRODUCTION

The use of polymers as food packaging materials has increased significantly over the past few decades. The global market for polymers has increased from approximately 5 million tonnes in the 1950s to nearly 100 million tonnes today. The packaging industry which constitutes almost 2% of the Gross National Product in some developed countries uses approximately 42% of the polymers worldwide.[1–4] Most packaging films are polymers derived from petroleum because of its functional advantages, cost, and availability.[5,6] Petroleum-based polymers have salient features such as strength, flexibility, stiffness, barrier to oxygen and moisture, and resistance to food component attack. However, their resistance to degradation and their recycling and disposal difficulties are very challenging in today's heightened strong global interest in environmentally sustainable materials.

Bioplastics are plastic polymers manufactured from renewal resources. Biopolymers are particularly attractive because they are biodegradable due to their susceptibility to microbial enzyme degradation. Bioplastics are being introduced into the market to serve as food packaging materials to primarily address concerns about plastic waste accumulation.[7–9] The bioplastics market is expected to grow between 20 and 25% until 2020.[10] The bioplastics growth in recent years is primarily attributable to the use of polylactic acid (PLA), a thermoplastic polymer that belongs to family of linear aliphatic polyesters derived from renewable resource (corn starch, tapioca roots, sugarcane, etc).[11] Although the biodegradable polymers present significant commercial potential for bioplastics, some of their properties such as brittleness, low heat distortion temperature, high gas permeability, and low melt viscosity for further processing may restrict their use for packaging.

Nanotechnology provides innovative improvements for plastics (petroleum based and bioplastics) in terms of polymer performance, cost, and environmental compatibility. Barrier properties, reduced energy inputs for production, transport and storage, reduction in waste volumes, and reduced carbon dioxide emissions are some of the nanotechnology-driven improvements.[12–18] For example, reinforcement of pristine PLA with nanoparticles has already shown to improve mechanical and barrier properties.[11,12,18] Improving the properties of such

biopolymers by nano reinforcements is therefore an attractive way to produce ecosustainable materials with very good potential for food packaging applications.

Food processing by ionizing radiation technologies such as cobalt-60, electron beam (eBeam), and X-rays is approved in all continents and in commercial use over 60 countries.[19–22] The radiation methodology has been endorsed as safe for foods and health by the World Health Organisation and the European Food Security Agency, that found there are no health risks for the consumer linked to the use of food irradiation.[23,24] The extent of clearances in the countries is varying from almost any food in Brazil to selected items in several EU countries, as listed by Official Journal of the European Union.[25] In US between 2007 and 2013, the total volume of commodities treated by ionizing radiation increased by over 6000% from 195,000 kg in 2007 to approximately 13 million kg in 2013.[20]

Food irradiation can be broadly divided into two categories based on the doses that are employed, namely, doses ≤ 1.0 kGy and doses ≤ 10 kGy. Doses ≤ 1.0 kGy are used primarily for eliminating insects and pests from fruits and vegetables and for extension of shelf-life, and doses ≤ 10 kGy for eliminating microbial pathogens from meat and poultry products. The use of doses ≤ 1.0 kGy for phytosanitary treatment of fruits and vegetables in international trade is the fastest growing market sector. Electron beam (eBeam) technology relies on the use of electricity to generate energized electrons as ionizing radiation. The salient features of eBeam processing are that it does not involve radioactive isotopes and the process is very quick and cost-effective. The number of eBeam processing facilities has grown to 1500 worldwide and has now outnumbered gamma irradiation facilities by almost 10:1. Most recent estimates suggest that eBeam systems account for approximately US $80 billion of added value to commercial products.[21,22] Plastic packaging is widely used in products that undergo either the $\leq$1.0 kGy or the $\leq$10 kGy dose scenarios.

So to contribute ensuring worldwide food quality, quantity, and safety in an eco-sustainable way, the challenge is now to synergistically exploit the improvements in the biopolymer packaging performance due to nanotechnology with the drastic reduction of microbial contamination on food following irradiation procedures.[21,26]

The aim of this study was two-fold: 1) to develop new films based on PLA/MMT with improved properties for applications in the food packaging industry and 2) to examine the effect of eBeam irradiation at two specific target doses (1 and 10 kGy) on the structural, morphological, mechanical, and barrier properties of these nanomaterials.

To improve the properties of PLA, a modified montmorillonite (MMT) was used as nanofiller. MMT is hydrated aluminasilicate-layered clay consisting of an edge-shared octahedral sheet of aluminum hydroxide between two silica tetrahedral layers.[27] MMT is relatively inexpensive and widely available natural clay derived from volcanic ash/rocks. To improve the homogenization of the nanoparticles in the polymer matrix, MMT was modified by substituting inorganic cations of MMT with organic ammonium ions.[28,29]

Table I. Composition of the PLA-Based System

Sample	PLA (wt %)	D67G (wt %)
PLA	100	0
PLA/D67G 1%	99	1
PLA/D67G 3%	97	3
PLA/D67G 5%	95	5

The two doses, namely 1 kGy and 10 kGy, and the control, 0 kGy, were employed in this study. The rationale for choosing these specific doses was that (as mentioned above) 1 kGy is approved by the US FDA to be used on all fresh produce in the United States for extending the shelf-life of fruits and vegetables. Given the high market value for fresh produce and since biopolymers can serve as packaging materials for fruit- and vegetable-based healthy vending machine items and for pediatric cancer patients,[30] it was decided that 1 kGy should be a target dose. The maximum dose that was employed was 10 kGy because this dose limit is at the upper limit for all foods that can be treated with irradiation in the US. The decision to focus on these two critical dose points can significantly improve the chances of these research findings to be commercially exploited.

EXPERIMENTAL

Materials and Sample Preparation

The organoclay (Laviosa, Livorno, Italy) is commercially available as Dellite 67G. Dellite 67G (D67G) is an organoclay derived from natural MMT modified with a high content of quaternary ammonium salt, in particular, dimethyl deydrogenated tallow ammonium. The polylactic acid (PLA 4032D) (Nature Works®) has $Mw = 1.3 \times 10^5$, $Mn = 2.1 \times 10^5$ (measured by Gel Permeation Chromatography, $Mw/Mn = 1.56$, $T_g = 58°C$, and $T_m = 160°C$ (measured by differential scanning calorimetry (DSC)). Before blending, PLA was vacuum dried (24 h, 80°C).

Masterbatch with clay content 20 wt % and PLA content 80 wt % was prepared to improve the dispersion of clay in the PLA by using a 25-mm twin screw co-rotating extruder *Collin ZK 25* ($L/D = 24$). The temperature setting of the extruder from the hopper to the die was 150/170/170/170/160°C, and the screw speed was 25 rpm.

PLA-based composites with 1, 3, and 5 wt % of clay were prepared by using the same extruder and conditions (see Table I). No compatibilizer was used when mixing nanoclay and PLA.

PLA/MMT films were obtained by a single-screw extruder *Collin E 20T* with a calender termination *Collin CR 72T*. The temperature setting of the extruder from the hopper to the die was 160/170/170/170/180°C, and the screw speed was 40rpm. The calender chill roll diameter and width were 72 and 190 mm, respectively. For the calender terminator, the temperature was set at room temperature and the load capacity of the double jacket roll and of the winder roll was set at 83 and 55 N, respectively. The thickness of the films obtained was about 50 μm.

eBeam Irradiation

The eBeam irradiation of the films was carried out at the eBeam facility of the National Center for Electron Beam Research at

Texas A&M University. A 10 MeV, 18 kW linear accelerator (downward orientation) was used. The film samples were placed in polyethylene holders which were taped to a solid support to ensure that they remained perfectly flat during eBeam processing. The processing was performed at room temperature (25°C). Alanine films (Kodak) were placed below the samples in order to measure the delivered eBeam dose. The film dosimeters were measured using a Bruker E-scan spectrometer (Bruker, Billerica, MA). The dosimetry was traceable to international standards. Two target doses were delivered, namely, 1 and 10 kGy. The measured doses were 1.02 ± 0.04 and 10.05 ± 0.18, respectively. The dose rate was approximately 1000 Gy/s. Replicate samples were subjected to two different (1 and 10 kGy) of eBeam doses. An unirradiated sample (0 kGy) was also included in these trials.

Characterization

Attenuated Total Reflectance (ATR) Spectroscopy Analysis. ATR spectroscopy was used to analyze the chemical structure of the irradiated and nonirradiated samples. The eBeam-treated and -untreated film samples were analyzed with a Perkin Elmer Spectrum 100 (resolution of 4 cm^{-1}, in a range of wave number from 4000 to 400 cm^{-1} and with a number of scans equal to 8) to highlight the possible formation of chemical species as a result of eBeam processing.

Wide-Angle X-ray Diffraction Analysis. Wide-angle X-ray diffraction (WAXD) measurements were performed using a Philips XPW diffractometer with Cu Ka radiation (1.542 Å) filtered by nickel. The scanning rate was 0.02° s^{-1} and the scanning angle was from 2.0 to 45°. The ratio of the area under the crystalline peaks and the total area multiplied by 100 was taken as the crystalline percentage degree.

Transmission Electron Microscopy. Morphological analysis was performed using a TEM, FEI Tecnai G12 Spirit Twin with emission source LaB6 using spot size 1. The micrographs were acquired with CCD camera Fei Eagle 4000 × 4000.

Thermal Analysis. The thermal behavior of the blends was examined by DSC using a calorimeter Mettler DSC-822. DSC measurements were carried out by (1) heating from −30°C temperature to 200°C at a rate of 10°C min^{-1}; (2) maintaining for 5 min at 200°C; (3) cooling to −30°C at 30°C min^{-1}; (4) maintaining for 2 min at −30°C; and (5) heating from −30 to 200°C at a rate of 10°C min^{-1}. DSC studies revealed the thermal properties of the samples, such as transition temperature (T_g), cold crystallization temperature (T_c), and melting temperature (T_m).

Mechanical Tests. Dumbbell-shaped specimens were cut from the films and used for the tensile measurements. Stress–strain curves were obtained using an Instron machine (Model 4505) at room temperature (25°C) at a cross-head speed of 2 mm min^{-1}. Twenty tests were performed for each composition.

Permeability Tests. Permeability to oxygen was tested on films by means of an ExtraSolution Multiperm apparatus. The instrumental apparatus consists of a double chamber diffusion cell. The film was inserted between the two chambers: a nitrogen flux containing oxygen enters in the lower one and a dry nitrogen flux flows in the upper one. A zirconium oxide sensor measures the oxygen diffusion across the film. The exposed area of the film was 50 cm^2. The sensor data was converted into oxygen transmission rate (OTR) (i.e., the oxygen flow rate between two parallel surfaces under steady conditions and specific temperature and relative humidity (RH)). Measurements were carried out in triplicate at 23°C and 0% RH. Oxygen permeability was calculated from OTR data by means of the following equation:

$$\text{Permeability} = (\text{OTR} \times \text{thickness})/\Delta P$$

where ΔP is the partial pressure between the two chambers of the instrument.

RESULTS AND DISCUSSION

ATR Spectroscopic Analysis

The samples were subjected to ATR spectroscopic analysis to highlight the presence of new chemical bonds due to the inclusion of the nanofiller within the polymer matrix and to eBeam irradiation exposure. The ATR spectra before and after exposure to eBeam doses of 1 and 10 kGy are shown in Figure 1.

eBeam irradiation of the film samples did not cause any changes in the chemical structure of the samples. This suggests that no new chemical bond formation would occur during eBeam processing at doses routinely used in food irradiation.

Structural and Morphological Analysis

The morphology and structure of the samples were analyzed using TEM and WAXD (Figures 2–7). Figure 2(a,b) shows the results of TEM and WAXD from pure clay samples. The TEM micrograph [Figure 2(a)] reveals that the powdered clay consists of lamellar stacks of rectangular shapes and that they are composed of several layers spaced apart of about 3.5 nm. The WAXD profile of the pure clay reported in the range 2–10° 2θ presents three peaks at 2.55° ($d = 3.4$ nm), 4.83° ($d = 1.8$ nm), and 7.25° ($d = 1.2$ nm) corresponding to the (001), (002), and (003) planes, respectively. These results indicate the presence of a multilayer structure. Specifically, the peak at 7.25° 2θ reflects the pristine MMT interlayer distances, indicating that the quaternary ammonium salt modification of the clay is not complete, whereas the other two peaks indicate that the modification generated two main interlayer distances.[31]

For the nanocomposites, the diffraction patterns at low 2θ values give information about the possible occurrence of intercalated/exfoliated clay structures of the clay due to PLA molecules penetrating the clay galleries.

For the nanocomposites, the peak at 2.55° 2θ was absent (Figure 3). The disappearance of this peak could indicate that the systems were intercalated/exfoliated. The WAXD results, primarily at low angle, could be misinterpreted due to sample orientation and/or poor calibration of the instrumentation. Thus, morphological analysis using TEM was performed to draw reliable conclusions. TEM micrographs reported in Figures 4 and 5 show a homogenous dispersion of the clays in the polymer matrix for all compositions. The clay was oriented along the machine direction (indicated by the arrow). Lamellar stacks (average length ranging between 400 and 700 nm) were observed. Few of these stacks are

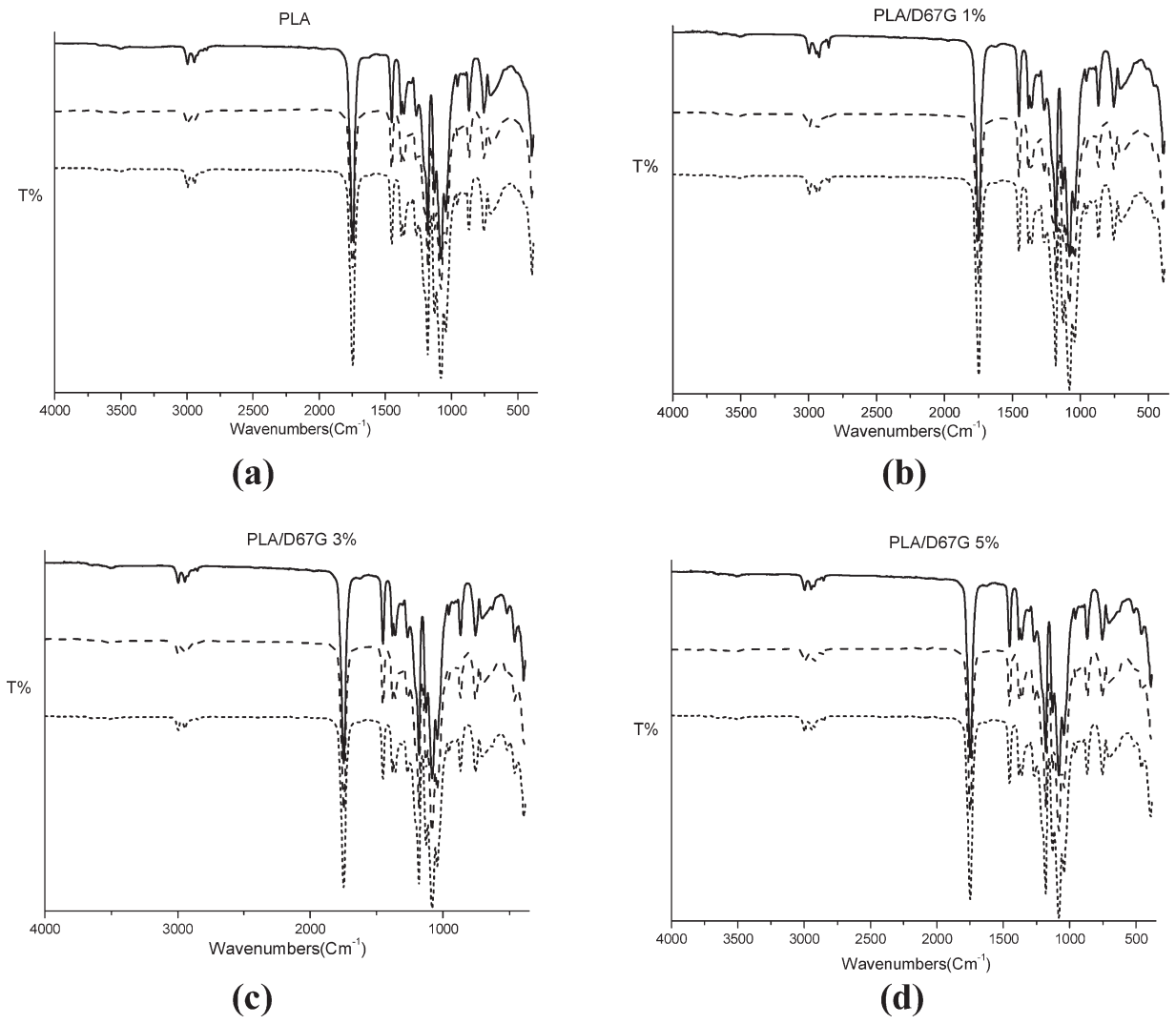

Figure 1. ATR spectra of the nanocomposites before and after exposure to eBeam doses of 1 and 10 kGy for (a) neat PLA, (b) PLA/D67G 1%, (c) PLA/D67G 3%, and (d) PLA/D67G 5%.

longer than 1 μm. The distance between the various layers that make up the clay stacks was measured from these images. In general, all the nanocomposites had larger interlayer distances compared to the pure clay powder which was approximately 3.5 nm. For the PLA/D67G 1%, the distance was approximately 8.0 nm; for the PLA/D67G 3%, it was approximately 9.0 nm; and for the PLA/D67G 5%, it was approximately 8.0 nm. The structural and morphological results reported here highlight some important findings: First, the extrusion process and subsequent calendering was able to create a good distribution and dispersion of the clay and PLA orientation in the matrix for the all tested compositions; second, the preparation process yielded a film containing an intercalated morphology with PLA macromolecules penetrating the clay galleries.[29,31,32]

Scanning electron micrographs (at 3000× magnification) of film surfaces of the samples before and after eBeam irradiation are shown in Figure 6. Prior to eBeam irradiation, the surface was smooth and homogeneous. After eBeam irradiation, the surface of the samples presented regions with higher roughness characterized by cavities and ripples of different size and shapes. The number and the size of both cavities and ripples increased in intensity between the 1 and 10 kGy exposed samples. It has been previously reported that ionizing radiation causes bond breakage in the PLA molecules and the formation of radicals that can recombine with each other.[32–37] Mool and Vilas[36] have reported that PLA undergoes both chain scission and cross-linking probably due to the cleavage of the ester linkage (increase in COOH end groups) and hydrogen abstraction at the quarternary carbon atom sites. Using electron spin resonance, Nugroho *et al.* [3%] identified at least three kinds of radicals due to chain scission when PLA is exposed to ionizing radiation. They postulate that after PLA irradiation reactions such as chain transfer, termination or recombination could be occurring separately or simultaneously. So it appears that ionizing irradiation can cause both the reduction of the molecular masses, due to degradation of the polymer, and the formation of cross-links between the chains with the consequent increase of the molecular masses. However, the creation of surface

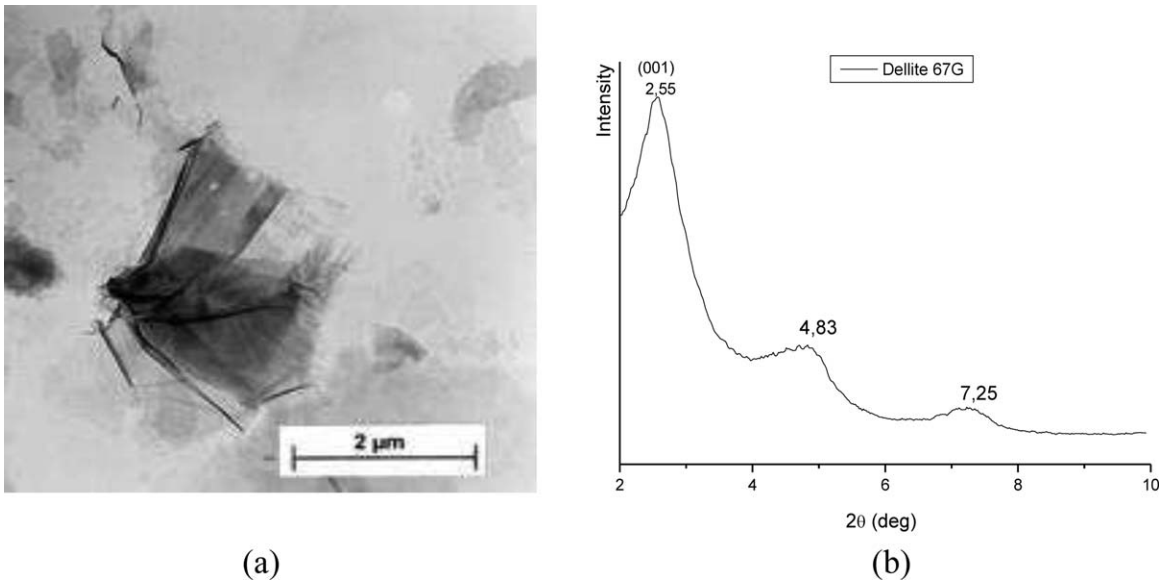

Figure 2. Pure clay when examined by (a) TEM micrograph and (b) wide-angle X-ray diffraction (WAXD).

roughness at doses as low as 1 kGy is very surprising and is worthy of further investigation.

Crystallinity

In order to investigate the presence and amount of crystallinity and the crystalline form of PLA crystals in the samples as obtained by the preparation process, WAXD analysis has been performed. Figure 7 shows the WAXD profiles for the unexposed and exposed nanocomposites to 1 and 10 kGy eBeam irradiation. Before the irradiation, both neat PLA and PLA/D67G 1% nanocomposite are completely amorphous, while a small amount of crystalline phase develops for the samples containing 3 and 5% of clay. In particular, the crystallinity for these two systems increases with the clay content (Table 2). The clay acting as a nucleating agent for the PLA crystal is in agreement with published literature.[10,12] The peaks at 17° and 19° 2θ suggest that PLA crystallizes in α form.[7] From the diffraction profiles (Figure 7), it is possible to conclude that the pure PLA remains amorphous also after the irradiation. For the nanocomposites, however, the X-ray diffraction pattern shows the formation of few crystals of the α-form for PLA/D67G 1% and increasing in crystallinity for the 3 and 5% nanocomposites of D67G.

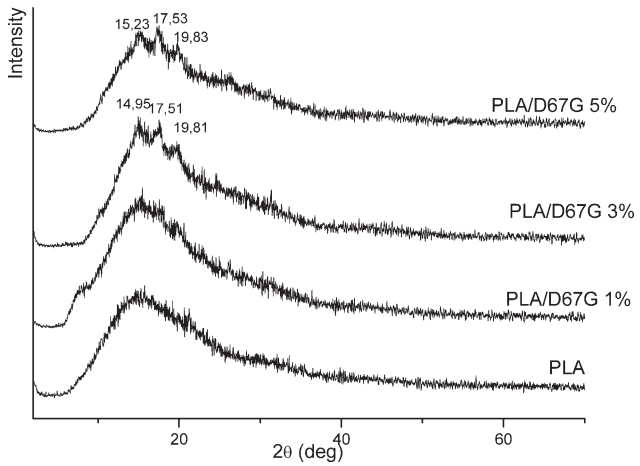

Figure 3. WAXD profile of neat PLA and nanocomposites.

Thermal Analysis

Figure 8 reports the thermograms of the samples, in the temperature range from 40 to 200°C, before and after the irradiation. In each figure, the curves are offset along the *Y*-axis to illustrate the trends. The calorimetric parameters are summarized in Table III. The curve of the pure PLA [Figure 8(a)] presents three transitions: an endothermic glass transition at 61°C; an exothermic cold crystallization peak that extends from about 85 to 115°C whose maximum, taken as the temperature of cold crystallization (T_c), is 100°C; and an endothermic melting peak which extends from about 155 to 175°C whose maximum, taken as the melting temperature (T_m), is 169°C. Thermoanalytical curves of nanocomposites before the irradiation do not show significant changes compared to pure PLA. These observations suggest that the clay at the composition used in these studies does not influence the cold crystallization of PLA, its melting, and nor does it alter the glass transition temperature. These results are in agreement with those reported in the literature.[33–35]

Thermoanalytical curves of nanocomposites and the calorimetric parameters after exposure to eBeam irradiation are also shown in Figure 8 and Table III, respectively. From the curves and the summarized parameters, it appears that eBeam irradiation produces a slight increase (about 4°C) in the T_g, in pure PLA and nanocomposites. This increase could be due to the formation of some cross-links between the chains, caused by the irradiation with the consequent increase of the molecular masses. When forming cross-links, the polymer chains are less mobile and this brings to an increase in the T_g.[35] The other

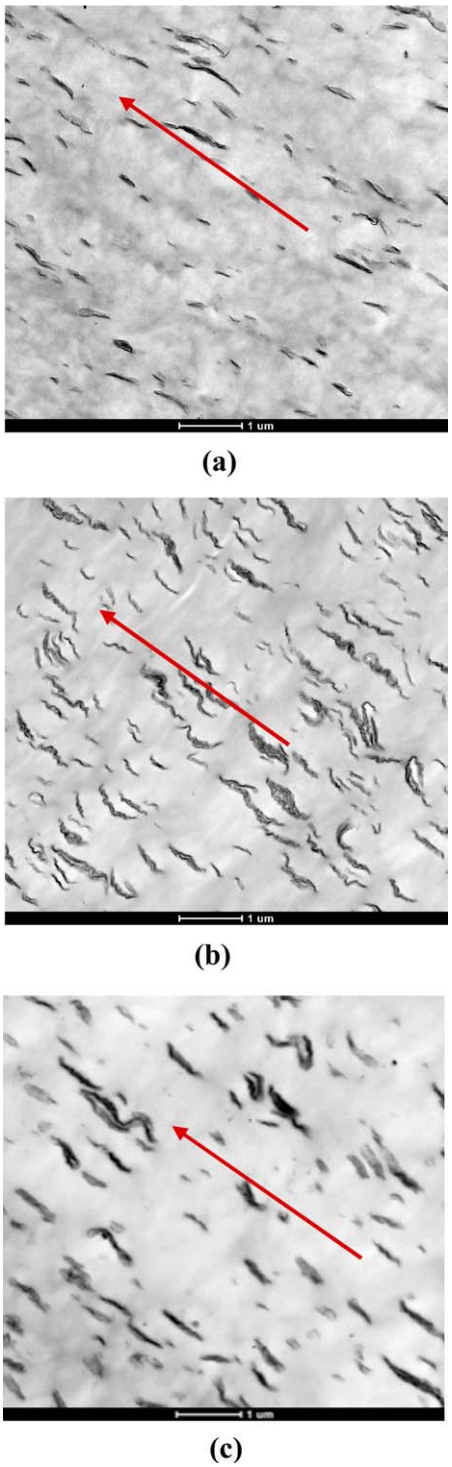

Figure 4. TEM micrographs of the nanocomposites (a) PLA/D67G 1%, (b) PLA/D67G 3%, and (c) PLA/D67G 5%. [Color figure can be viewed in the online issue, which is available at wileyonlinelibrary.com.]

thermal characteristics, T_m and T_c, however, do not appear to be influenced by exposure to eBeam radiation.[38]

Tensile Properties

The PLA always shows a plastic behavior with the phenomenon of yield, fiber elongation, and final breaking (see Figure 9 for example). The mechanical parameters [Young's modulus (E), stress and deformation (σ_y, ε_y) at yield, and stress and deformation (σ_b, ε_b) at break] in the machine direction and in the transverse direction for all samples are reported in Tables IV and V. The mechanical properties of the untreated PLA are in agreement with those reported in the literature.[36–38] The nanocomposites exhibit the same trend as the neat PLA. Although due to the quite large scatter in the results (see Tables IV and V), it is challenging to clear conclusions, the data obtained could give indication of the following trends. For the nonirradiated samples, the addition of clay seems to cause an improvement in the values of the modulus (E) and deformation at break (ε_b), and a reduction of σ_b. It should be noted that the yield strength parameters (ε_y, σ_y) are not strongly influenced by the presence of clay. For the eBeam-treated samples, the treatment seems to cause some changes in the tensile properties. In particular, it is found, at a given composition, an increase of E, σ_b, and σ_y for all the samples analyzed (with the only exception being PLA 1 kGy), in both directions and for both doses of radiation. Conversely, the elongation at break in the samples treated with the eBeam is reduced when the eBeam dose is increased from 1 to 10 kGy. From Tables IV and V, it can be seen that for a given direction, ε_y is not influenced by the irradiation treatment.

In general, the increase of the stress at yield and break, elastic modulus, and decrease in elongation at break are found in materials which undergo cross-links. Therefore, the results reported here could suggest that in the neat PLA and PLA nanocomposites, during eBeam irradiation, there is the formation of cross-links among the PLA chains. It is not excluded that this process is also accompanied by degradation with formation of shorter molecular chains. However, further detailed studies are needed to understand why these processes occur at low doses such as 1 kGy. The comparison of the values of the mechanical parameters for the two directions indicates that in the machine direction, the samples seem to behave better than in transverse direction confirming the structural anisotropy observed through the morphological analysis.

BARRIER PROPERTIES

The OTR and permeability values as a function of composition and eBeam dose are shown in Table VI. For the nonirradiated samples, the barrier properties depend on the composition. Compared to the neat PLA, the PLA/D67G composites show up to a 32% improvement in the barrier properties as seen in the PLA/D67G 5% composition.

It is known that permeability of a composite polymer depends on a variety of factors. The permeability results could be interpreted as follows: first, an increase in the crystalline phase (considered to be impermeable to gas) should lower the permeability; second, the presence of clay particles, especially if dispersed in nanometric and micrometric dimensions, could alter the path of the permeating gas molecules which are forced to travel a longer path through the film; and third, the influence of other factors such as the interface structure (degree of adhesion between the phases and free volume at the interface) should be taken into consideration.[39]

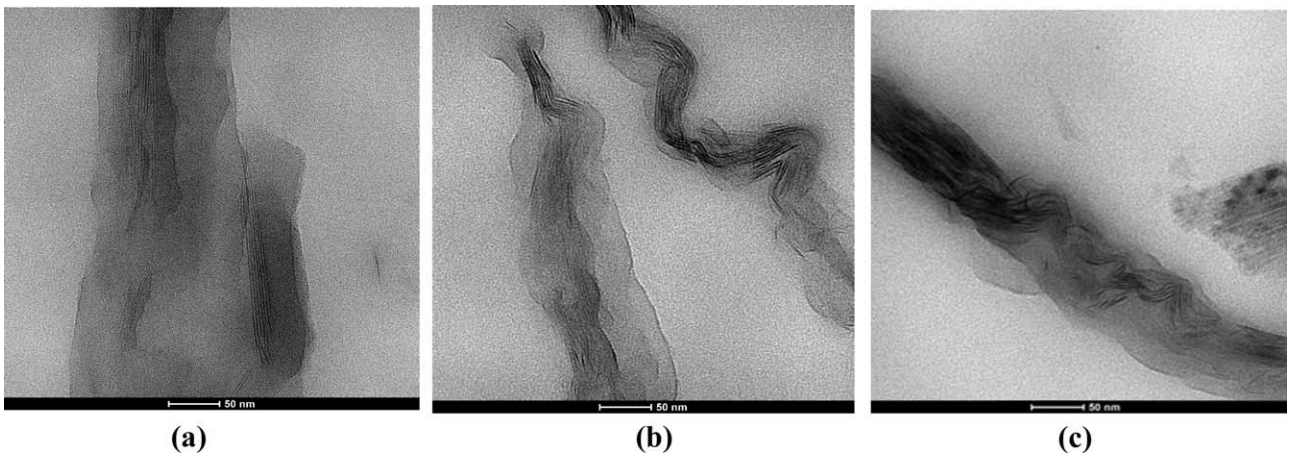

Figure 5. TEM micrographs at higher magnifications for (a) PLA/D67G 1%, (b) PLA/D67G 3%, and (c) PLA/D67G 5%.

Sample	0 kGy	1 kGy	10 kGy
PLA	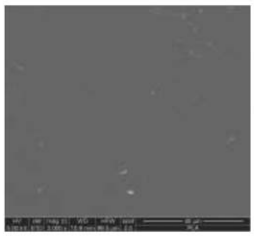	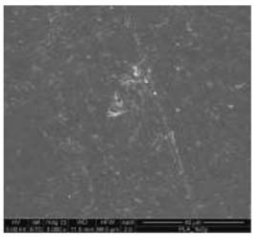	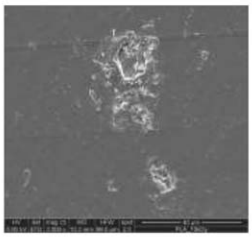
PLA-1%	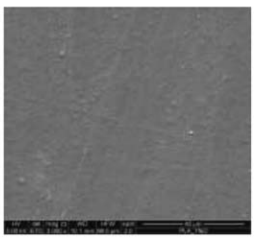	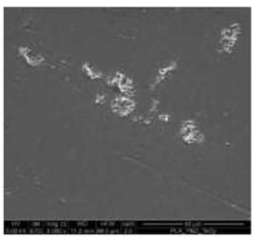	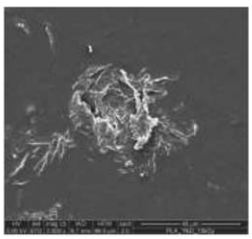
PLA-3%	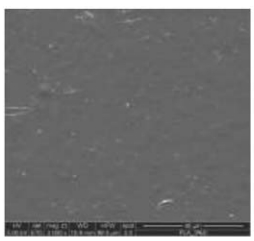	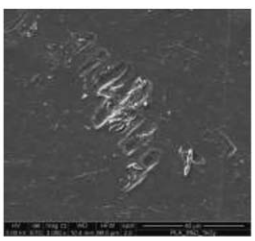	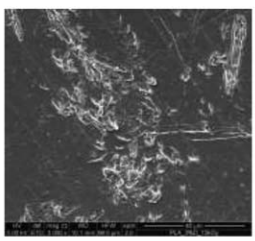
PLA-5%	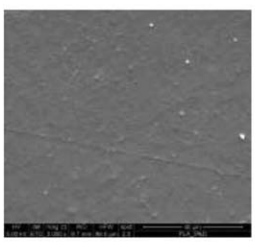	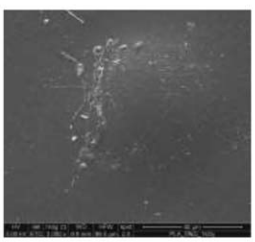	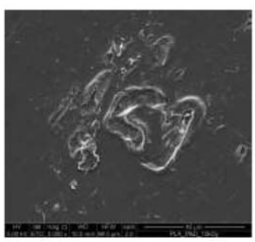

Figure 6. Scanning electron micrographs (3000× magnification) of films surfaces of the samples irradiated at 1 and 10 kGy.

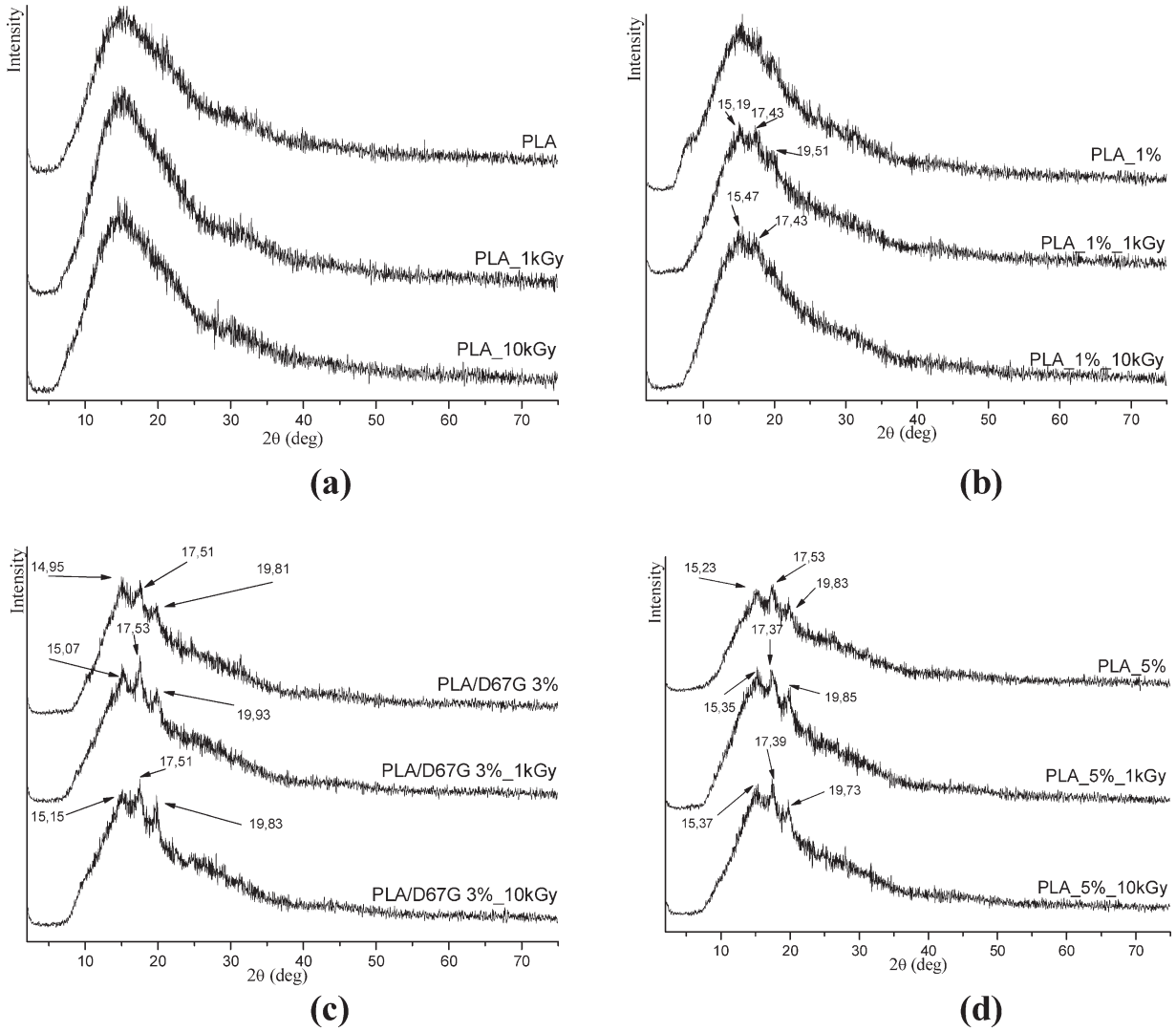

Figure 7. WAXD profile of the (a) neat PLA and the PLA/D67G nanocomposites before and after exposure to 1 and 10 kGy eBeam doses.

The decrease of permeability observed for the nanocomposites could be attributed to an increase of the tortuous path that the O_2 molecules must travel within the film due to the presence of clay particles. Moreover, in the 3 and 5% PLA/clay nanocomposites, the crystallization of PLA (Table 2) could be contributing to further reduce the permeability. On the other hand, however, increasing the clay composition has shown to result in the presence of bigger clay agglomerates. These agglomerates prevent a more drastic reduction of the permeability especially in samples containing 5% D67G nanocomposites.

Table 2. Crystallinity Before and After Irradiation at 1 and 10 kGy

Sample	X_c (%)
PLA/D67G 1%	-
PLA/D67G 1%_1 kGy	2
PLA/D67G 1%_10 kGy	3
PLA/D67G 3%	4
PLA/D67G 3%_1 kGy	6
PLA/D67G 3%_10 kGy	5
PLA/D67G 5%	8
PLA/D67G 5%_1 kGy	9
PLA/D67G 5%_10 kGy	7

For the eBeam irradiated samples, the permeability for a given composition appears to depend on the irradiation dose. In particular, for the samples irradiated at 1 kGy, the permeability values decreased by about 4–5% compared to the untreated samples at a given composition. This decrease in permeability could be due to the increase in crystallinity and the formation of cross-links, which increase the rigidity of the amorphous phase. When the eBeam dose is increased to 10 kGy, the permeability increases compared to the 1 kGy treated samples and in some cases also with respect to those not treated. This result is probably due to the effect of the irradiation on the film surface that produced at the high irradiation deep cavities that facilitate the diffusion of gases (Figure 6).

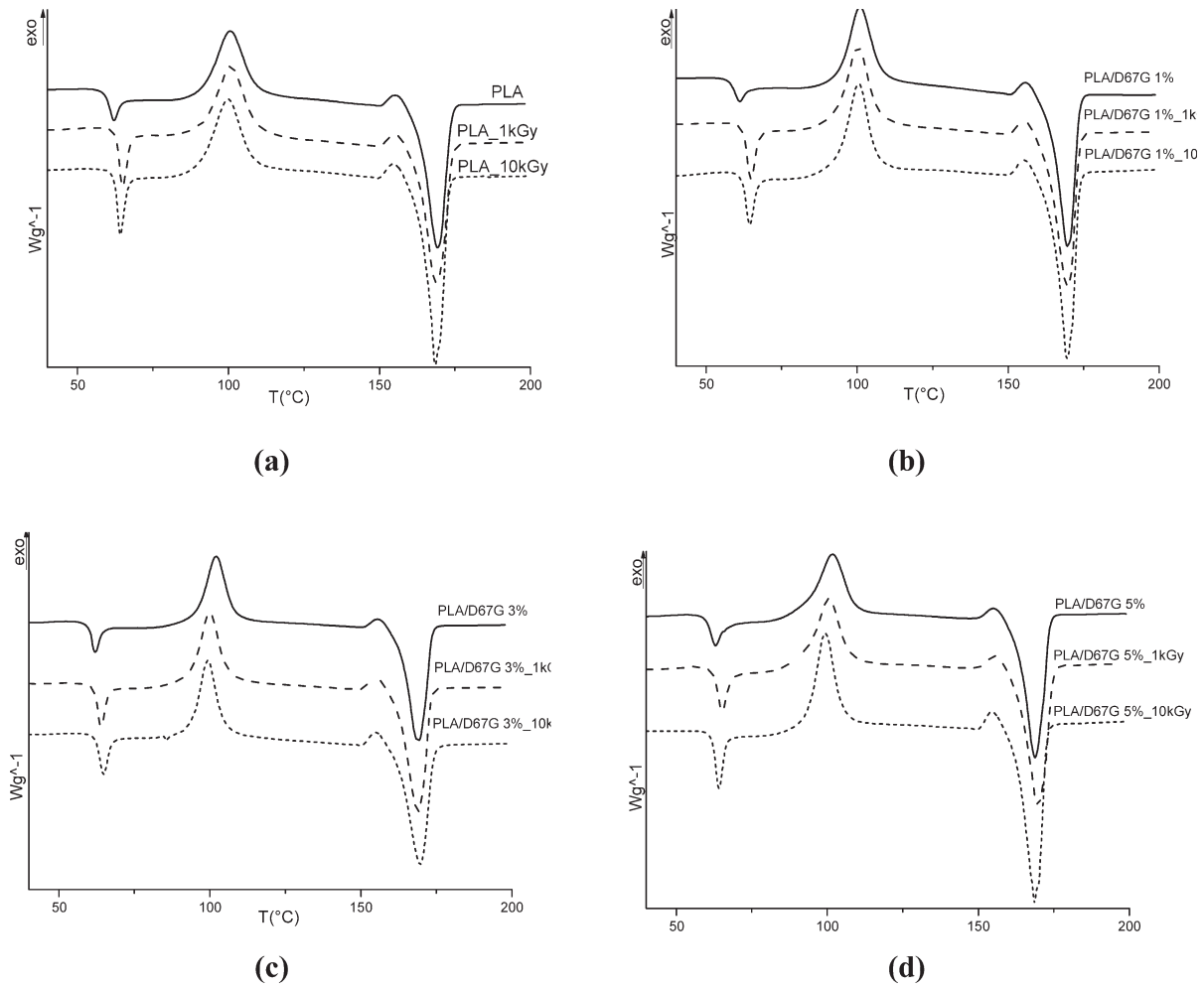

Figure 8. Thermograms before and after exposure to 1 and 10 kGy eBeam dose irradiation of (a) neat PLA, (b) PLA/D67G 1%, (c) PLA/D67G 3%, and (d) PLA/D67G 5%.

The use of nanomaterials as well as of radiation technologies applied to food is posing concerns on the health about indirect sources of food contamination by nanoparticles and radiolytic products formed in the packaging materials during the irradiation that could migrate to the food.[5,21]

Table III. Calorimetric Parameters Before and After Irradiation at 1 and 10 kGy eBeam Dose

Sample	T_g (°C)	T_c (°C)	T_m (°C)
PLA	61	100	169
PLA_1 kGy	64	100	169
PLA_10 kGy	63	100	169
PLA/D67G 1%	60	101	169
PLA/D67G 1%_1 kGy	64	100	169
PLA/D67G 1%_10 kGy	64	100	169
PLA/D67G 3%	61	102	169
PLA/D67G 3%_1 kGy	63	100	169
PLA/D67G 3%_10 kGy	64	100	169
PLA/D67G 5%	61	102	169
PLA/D67G 5%_1 kGy	64	100	169
PLA/D67G 5%_10 kGy	63	100	169

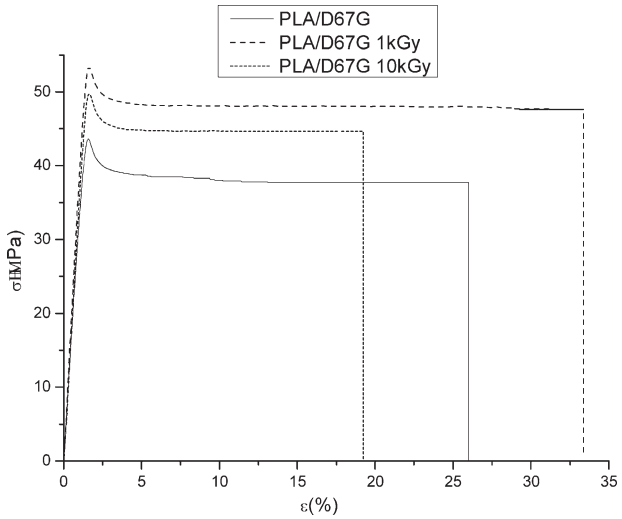

Figure 9. Stress–strain curves of neat PLA as a function of eBeam irradiation dose. Machine Direction.

Table IV. Tensile Parameters of the Samples Tested in Machine Direction

Sample	*E* (Mpa)	σ_y (Mpa)	ε_y (%)	σ_b (Mpa)	ε_b (%)
PLA	3469 ± 189	43.9 ± 1.7	1.6 ± 0.1	37.7 ± 1.7	25.7 ± 5.3
PLA_1 kGy	4092 ± 157	53.8 ± 3.5	1.6 ± 0.1	47.3 ± 2.5	33.3 ± 4.3
PLA_10 kGy	3794 ± 148	50.3 ± 3.2	1.6 ± 0.1	44.5 ± 2.7	19.2 ± 4.9
PLA/D67G 1%	3622 ± 372	40.0 ± 5.2	1.4 ± 0.2	33.8 ± 4.3	39.0 ± 5.8
PLA/D67G 1%_1 kGy	4061 ± 198	49.8 ± 3.4	1.5 ± 0.1	41.5 ± 4.0	56.9 ± 6.4
PLA/D67G 1%_10 kGy	3917 ± 217	46.0 ± 2.0	1.5 ± 0.1	40.5 ± 1.7	29.0 ± 4.2
PLA/D67G 3%	3529 ± 264	39.9 ± 2.7	1.4 ± 0.1	29.8 ± 1.7	41.2 ± 5.8
PLA/D67G 3%_1 kGy	4049 ± 284	41.9 ± 5.2	1.4 ± 0.1	33.0 ± 4.5	33.1 ± 6.5
PLA/D67G 3%_10 kGy	3999 ± 278	43.3 ± 3.1	1.4 ± 0.1	34.5 ± 3.2	15.2 ± 3.1
PLA/D67G 5%	3550 ± 152	38.3 ± 4.0	1.4 ± 0.2	30.2 ± 3.0	35.6 ± 9.8
PLA/D67G 5%_1 kGy	4136 ± 192	46.7 ± 3.0	1.4 ± 0.1	35.1 ± 3.3	40.1 ± 9.3
PLA/D67G 5%_10 kGy	4091 ± 206	49.1 ± 3.9	1.5 ± 0.1	37.8 ± 3.4	33.2 ± 5.6

Table V. Tensile Parameters of the Samples Tested in Transverse Direction

Sample	*E* (Mpa)	σ_y (Mpa)	ε_y (%)	σ_b (Mpa)	ε_b (%)
PLA	3376 ± 393	35.2 ± 2.5	1.3 ± 0.1	31.7 ± 1.9	10.0 ± 4.4
PLA_1 kGy	3846 ± 113	33.5 ± 3.5	1.1 ± 0.1	30.2 ± 2.8	5.0 ± 1.0
PLA_10 kGy	3601 ± 188	39.3 ± 3.3	1.3 ± 0.1	35.3 ± 3.0	4.2 ± 1.8
PLA/D67G 1%	3699 ± 207	33.7 ± 4.3	1.2 ± 0.1	29.7 ± 2.7	29.7 ± 5.1
PLA/D67G 1%_1 kGy	3972 ± 195	39.6 ± 3.3	1.3 ± 0.1	34.2 ± 3.0	23.8 ± 8.8
PLA/D67G 1%_10 kGy	3981 ± 268	41.2 ± 2.7	1.3 ± 0.1	35.5 ± 3.4	11.7 ± 2.6
PLA/D67G 3%	3578 ± 256	33.0 ± 4.4	1.2 ± 0.1	26.2 ± 3.6	31.1 ± 6.3
PLA/D67G 3%_1 kGy	4137 ± 241	39.9 ± 3.2	1.2 ± 0.1	31.8 ± 3.3	7.0 ± 1.78
PLA/D67G 3%_10 kGy	4394 ± 131	45.3 ± 3.8	1.3 ± 0.1	37.4 ± 2.8	5.0 ± 1.4
PLA/D67G 5%	3648 ± 228	35.6 ± 3.4	1.3 ± 0.1	28.8 ± 2.7	20.5 ± 5.6
PLA/D67G 5%_1 kGy	3859 ± 138	39.0 ± 5.2	1.3 ± 0.1	32.0 ± 4.1	10.8 ± 4.4
PLA/D67G 5%_10 kGy	4138 ± 67	43.1 ± 2.2	1.3 ± 0.1	34.7 ± 3.0	10.7 ± 1.8

Table VI. OTR and Permeability Values

Sample	OTR (cm^3/(24 h m^2))	Permeability (cm^3cm/m^2 24 h 100 kPa)
PLA	573	2.23 ± 0.22
PLA_1 kGy	519	1.61 ± 0.01
PLA_10 kGy	539	1.78 ± 0.04
PLA/D67G 1%	458	1.76 ± 0.01
PLA/D67G 1%_1 kGy	441	1.52 ± 0.01
PLA/D67G 1%_10 kGy	455	1.64 ± 0.08
PLA/D67G 3%	385	1.52 ± 0.03
PLA/D67G 3%_1 kGy	358	1.43 ± 0.09
PLA/D67G 3%_10 kGy	390	1.58 ± 0.05
PLA/D67G 5%	380	1.52 ± 0.07
PLA/D67G 5%_1 kGy	374	1.46 ± 0.01
PLA/D67G 5%_10 kGy	403	1.63 ± 0.08

In order to improve the consumers perception about the application of the nanotechnology and radiation to food and to favor the market penetration of the new materials, migration testing after irradiation of PLA/MMT-based films by using food simulants is under investigation as function of composition and irradiation dose and will be reported in a forthcoming paper.

CONCLUSIONS

The goal of this project was to develop new films based on PLA and MMT with improved barrier and mechanical properties. These were designed for use with foods being processed with eBeam technology for shelf-life extension, phytosanitary treatment, and pathogen elimination. Hence, only doses $\leq$1 and $\leq$10 kGy were employed. Nanocomposite films were prepared at 1, 3, and 5% by weight of clay and exposed to target eBeam doses of 1 and 10 kGy. The samples were characterized by WAXD, TEM, ATR, SEM, DSC, TGA, tensile properties, and barrier properties before and after

eBeam irradiation at 1 and 10 kGy. The results show that the process of extrusion and subsequent calendering used to prepare the films was able to create a homogeneous dispersion of the filler in the organic matrix, with a relevant intercalation of PLA into the clay galleries. Moreover, it was observed that PLA properties are influenced by the addition of clay and by eBeam irradiation treatment. In particular, it was found that after eBeam exposure, the samples showed some surface irregularities, increases of T_g and Young modulus, and decrease of oxygen permeability. These results were attributed to the presence the clay which creates a tortuous path for oxygen migration through the film, to cross-link formation following eBeam exposure, and to increase in crystallinity following the addition of clay and the eBeam processing. These results lead to the conclusion that the PLA-based nanocomposites not only offer improved barrier and mechanical properties with respect to the pure PLA but also can be customized for different applications that are needed in the food processing industry.[40]

ACKNOWLEDGMENTS

The authors acknowledge the support from the IAEA Coordinated Research P F22063, Italy/Quebec Joint project n. PGR01085 and Cost Action FA0904.

REFERENCES

1. Selke, S. E. M.; Culter, J. D.; Hernandez, R. J. Plastics Packaging: Properties, Processing, Applications, and Regulations, 2nd ed.; Carl Hanser Verlag: Munich, DE, **2004**.
2. Robertson, G. L. Food Packaging: Principles and Practice, 2nd ed.; CRC Press: Boca Raton, FL, **2006**.
3. Marsh, K.; Bugusu, B. *J. Food Sci.* **2007**, *72*, R39.
4. Coles, R.; McDowell, D.; Kirwan Mark, J. Food Packaging Technology; CRC: Boca Raton, FL **2003**.
5. Silvestre, C.; Cimmino, S. Ecosustainable Polymer Nanomaterials for Food Packaging; CRC: Boca Raton, FL, **2013**.
6. Cimmino, S.; Duraccio, D.; Silvestre, C.; Pezzuto, M. *Appl. Surf. Sci.* **2009**, *256*, S40.
7. Ahmed, J.; Varshney, S. K. *Int. J. Food Prop.* **2011**, *14*, 37.
8. Sin, L. T.; Rahmat, A. R.; Rahman, W. A. Polylactic Acid: PLA Biopolymer Technology and Applications; William Andrew-Elsevier Publishing: Amsterdam, NL, **2012**.
9. Jamshidian, M.; Tehrany, E. A.; Imran, M.; Jacquot, M.; Desobry, S. *Food Sci. Food Saf.* **2010**, *9*, 552.
10. Helmut Kaiser Consultancy. Bioplastics Market Worldwide 2014-2015-2020-2025 and historical dates 2011-12-13 Applications, methods, competition, materials, technologies, development Recycling, renewable energy, Production, Consumption. Available at: http://www.hkc22.com/bioplastics.html. Accessed on March, 27, 2015.
11. Krikorian, V.; Pochan, D. *J. Chem. Mater.* **2003**, *15*, 4317.
12. Rhim, J. W. *Food Sci. Biotechnol.* **2007**, *16*, 691.
13. Sorrentino, A.; Gorrasi, G.; Vittoria, V. *Trends Food Sci. Technol.* **2007**, *18*, 84.
14. Silvestre,C.; Duraccio, D.; Cimmino, D. *Progr. Polym. Sci.* **2011**, *36*, 1766.
15. Duraccio, D.; Silvestre, C.; Pezzuto, M.; Cimmino, S.; Marra, A.; In Ecosustainable Polymer Nanomaterials for Food Packaging; Silvestre, D. C.; Cimmino, S., Eds.; CRC Press: Boca Raton, **2013**.
16. Arora, A; Padua, G. W. *J. Food Sci.* **2010**, *75*, R43.
17. de Azeredo, H. M. C. *Food Res. Int.* **2009**, *42*, 1240.
18. Weiss, J.; Takhistov, P.; McClements, D. J. *J. Food Sci.* **2006**, *71*,107.
19. Farkas, J.; Farkas, C. M. *Trends Food Sci. Technol.* **2011**, *22*, 121.
20. Cleland, M. R.; In Advances in Gamma Ray, Electron Beam, X-Ray Technologies for Food Irradiation in Food Irradiation Research and Technologies; Sommers, C. H.; Fan., X. Eds.; Blackwell Publ.: Oxford, **2006**.
21. Pillai, S.; Shayanfar, S. Electron Beam Pasteurization and Complementary Food Processing Technologies; Woodhead Publishing: Cambridge, UK, **2015**.
22. Pillai, S. D.; Braby, L. A.; Lavergne, C. B. In The International Review of Food Science and Technology. International Union of Food Science and Technology (IUFoST), Winter 2004/2005 Issue; Ottaway, P. B., Ed.; Sovereign Publications Limited: London UK, **2015**.
23. WHO technical report series: 890 1. Food radiation 2. No-observed-adverse-effect level 1. Title II- Series ISBN 924 120890 2 (Classification NLM: WA 710) ISSN 0512–3054.
24. EFSA Journal 2011; 9(4):2013 EFSA Panel on Biological Hazards (BIOHAZ) Scientific Opinion on Irradiation of food (efficacy and microbiological safety), doi: 10.2903/j.efsa.2011.2013. Available at: online: www.efsa.europa.eu/efsajournal. Accessed on March 27, 2015.
25. Official Journal of the European Union C 283/5 24.11.2009. doi:10.3000/17252423.C_2009.283.eng. Available at: http://eur-lex.europa.eu/legal-content/EN/TXT/?uri=OJ:C:2009:283:TOC. Accessed on March, 27 2015.
26. Silvestre, C.; Pezzuto, M.; Duraccio, D.; Marra, A.; and Cimmino, S. In: Radiation Processed Materials in Products from Polymers for Agricultural Applications. International Atomic Energy Agency: Vienna, **2014**.
27. Paiva, L. B.; Morales, A. R.; Diaz, F. R. V. *Appl. Clay. Sci.* **2008**, *42*, 8.
28. LeBaron, P. C.; Wang, Z.; Pinnavaia, T. *J. Appl. Clay Sci.* **1999**, 11.
29. Shi, Hengzhen; Lan, Tie; Pinnavaia, T. *J. Chem. Mater.* **1996**, *8*, 1584.
30. Smith, B.; Shayanfar, S.; Pillai, S. D. Synergistic Enhancement of Quality Attributes of Strawberries by Combining Modified Atmosphere Packaging and Electron Beam (eBeam) Processing for Foods Targeting Cancer Patients. *IFT Annual Meeting. New Orleans* **2014**.
31. Beermann, T.; Brockamp, O. *Clay Miner.* **2005**, *40*, 1.

32. Ho, Kai-Lai G.; Pometto III, A. L. *J. Environ. Polym. Degrad.* **1999**, *7*, 93.

33. Chrissafis, K.; Paraskevopoulos, K. M.; Papageorgiou, G. Z.; Bikiaris, D. N. *Appl. Polym. Sci.* **2008** *110*, 1739.

34. Mool, C. G.; Vilas., G. D. *Polymer* **1983**, *24*, 827.

35. Nugroho, P.; Mitomo, H.; Yoshii, F.; Kune, T. *Polym. Degrad. Stab.* **2001**, *72*, 337.

36. Quynh, T. M.; Mitomo, H.; Nagasawa, N.; Wada, Y.; Yoshii, F.; Tamada, M. *Eur. Polym. J.* **2007**, *43*, 1779.

37. Bee, S. T.; Ratnam, C. T.; Sin, L. T.; Tee, T. T.; Wong, W. K.; Lee, J. X.; Rahmat, A. R. *Nucl. Instr. Methods Phys. Res. Sect B: Beam Interact. Mater. Atoms* **2014**, *334*, 18.

38. Perego, G.; Cella, G. D.; Bastioli, C. *J. Appl. Polym. Sci.* **1996**, *59*, 37.

39. Nielsen, E. *J. Macromol. Sci. Part A Pure Appl. Chem.* **1967**, *1*, 929.

40. Zivanovic, S.; In Electron Beam Pasteurization and Complementary Food Processing Technologies; Pillai, S. D.; Shayanfar, S. Eds.; Woodhead Publishing: Cambridge, UK, **2015**.